

single [] tree

Deliverable 4.1

Single tree traceability



D4.1: Methodology for single tree traceability

Authors: Henrik Persson, Johan Holmgren, Petter Ideström, Carolin Fischer, Tuomas Yrttimaa, Nicolas Cattaneo, Stefano Puliti

Deliverable details

Contractual delivery date	Actual delivery date	Delivery type*	Dissemination level
31 Dec. 2025	30 Dec. 2025	R	P

*Delivery type: R: Document, report; DATA — data sets, microdata, etc; DEM — Demonstrator, pilot, prototype; DEC — Websites, patent filings, videos, etc; DMP — Data

Management Plan.

**Dissemination Level PU: Public; SEN: Sensitive, limited under the conditions of the Grant Agreement.

Version History

Version	Date	Modified by	Action	Status	Dissemination level
1.0	21/11/2025	Henrik Persson	First draft	Draft	SEN
2.0	30/12/2025	Stefano Puliti	Final Version after internal review	Final	P

*Status: Draft, Final, Approved, Submitted (to European Commission).

Disclaimer

This document reflects only the authors' view and not those of the European Community. This work may rely on data from sources external to the members of the SingleTree project consortium. Members of the Consortium do not accept liability for loss or damage suffered by any third party because of errors or inaccuracies in such data. The information in this document is provided "as is" and no guarantee or warranty is given that the information is fit for any particular purpose. The user thereof uses the information at its sole risk and neither the European Community nor any member of the SingleTree Consortium is liable for any use that may be made of the information.

Keywords

Laser scanning; individual tree; traceability, fingerprint,

Executive Summary

Deliverable 4.1 consists of the methodology and preliminary results for tracing single trees using tree branch patterns as biometric fingerprints as means for uniqueness. The branch pattern is extracted from dense laser scanning data in the forest and matched to the corresponding branch pattern as extracted from CT scanner data from the sawmill in the other end of the value chain. Different sensors, forests, tree species and implementations have been tested. Automatic methods for single-tree traceability from tree location in the forest to products would make it possible to prove the origin of wood products and enable big data analysis connecting sawmill measurements from, e.g., X-ray based computer tomography (CT) data, with large amounts of remote sensing data of forests. Permanent marker methods like the Logscam system (np2.logscam.com) have been used to tag logs by machines for log traceability, a limitation that causes additional costs and reduces the applicability in all-weather-conditions. This report outlines the work of the SingleTree project task 4.1 that has developed a proof-of-concept relying on natural biometric features combined with position tracking to eliminate the need for additional equipment and allow traceability at scale.

single  tree

D4.1 Tracing single trees

Consortium

 **NIBIO**


SLU
SWEDISH UNIVERSITY
OF AGRICULTURAL
SCIENCES


UNIVERSITY OF
EASTERN FINLAND

 **iuFOR**
Instituto
Universitario de Investigación
GESTIÓN
FORESTAL
SOSTENIBLE

 **NLS**
FINNISH GEOSPATIAL
RESEARCH INSTITUTE
FGI

 **SCA**

 **CREATIVE
OPTIMIZATION**

KELLUU


**KOKO
FOREST**

cesefor
FORESTRY HEART, research spirit

 **NTNU**


WSL

 **SFB**
Staatsforstbetrieb
Kanton Bern

EFD
Entreprise Forêts
domaniales du
canton de Berne

PRS Photogrammetry
Remote Sensing
ETH zürich

1. Introduction

Forests are pivotal in mitigating climate change, conserving biodiversity, and supplying raw materials for the bio-economy. The forestry-wood conversion chain, from forest to final product. To accurately identify which attributes of a standing tree best align with the quality requirements of sawn timber, it is essential to connect forest-collected data with information from the sawmill. To achieve this, the traceability of tree-log-sawn timber information is a key aspect of linking the data to be used in the learning of prediction algorithms (Winberg et al. 2023). Traceability systems facilitate the tracking of resources across processing stages, optimizing decisions in management involving multiple industrial processes, including forest planting/regeneration, management, harvesting, log handling, sawing, sorting, drying, value-added processing, final manufacturing, and recycling of wood products. In this chain, outputs from each industrial phase serve as inputs for the next, making wood quality intimately tied to the specifications of the final production, cultivation, harvesting, and processing, with the ultimate aim of achieving optimal product quality. Ensuring traceability from forest to industry addresses the need to guarantee wood origin, fight against illegal logging, promote local, sustainable resources, and streamline material flow by better understanding wood characteristics. There are various possible approaches to enable tracing of single logs from the forest to the sawmill. The methods include, e.g., punching, barcoding, and DNA fingerprinting, but they all also face limitations in costs, feasibility at implementation, and weather conditions (Tzoulis et al 2013). Biometric characteristics, such as knot positions, annual rings, pith patterns, and cross-section images of log ends, provide alternative approaches for log identification (Chiorescu et al. 2003, Schraml et al. 2015). One of the most intuitive methods is visual tracing, where photographs of the stems are used to recognize the same logs in the sawmill, as when standing in the forest. Some limitations with this method are changes in log appearance due to dirt, damage, snow or damages due to log processing and transport.

Logs can look similar, making accurate identification difficult, especially in large-scale operations. It also lacks integration with digital systems and is prone to errors in matching or interpretation. Another method for visual tracing incorporates cross-sectional photographs (of the ends of the logs), recognizing the unique fingerprint of year ring data visible after the cut (Schraml et al. 2016, Holmström et al. 2023). This method offers unique identification through natural growth ring patterns, enabling non-invasive, cost-effective tracking and integration with image recognition software. However, it faces challenges like

obscured patterns from damage or dirt, altered surface during processing, high data storage needs, computational demands for large scale matching, and weather or lighting conditions may affect image quality in outdoor operations. The technical improvements in harvesters and recent extension of GNSS systems have enabled cut-to-length (CTL) harvesters to position the single trees with centimeter accuracy. This enables an approach that combines the GNSS position with the outer shape of trees, e.g., the length and dimension of logs constituting a tree, and allowing them to connect entire trees recognizable in the sawmill. It is a promising approach but requires precise GNSS devices for accurate location mapping and advanced imaging techniques. To reduce the technical requirements and increase the robustness of the tracing, we propose the use of branch pattern - the spatial relationship of branches of a tree - to constitute a unique fingerprint of the trees, that is easily accessible in computer tomography (CT) data at the sawmill. Yrttimaa et al. (2025) demonstrated that the arrangement of branches along the stem surface as characterized by terrestrial laser scanning can serve as a basis for individual tree identification. In a study conducted in a managed boreal forest stand (0.4 ha), they found that geometric patterns consisting of more than 10 branch origins could provide unique identifiers for Scots pine trees. This suggests that a link could be established between a point cloud-reconstructed tree and its CT-scanned logs if enough branch origins are accurately reconstructed and matched between the datasets. The uniqueness of branching arrangements may also suggest that each tree possesses a distinct crown architecture, where the directional and vertical distribution of branch and foliage mass (e.g. point cloud metaproperties as in (Cattaneo et al. 2024) could be linked with information obtained from CT scanning. Data for such observations might be more attainable over larger areas using close-range airborne laser scanning or ground-based mobile laser scanning integrated into forest machinery.

The objectives have been to develop an automatic method for single tree tracing based on LiDAR from the forest and CT scanner images at the sawmill. In the proof-of-concept state, it will allow tracing most of the logs. As the approach is more widely applied, the amounts of training data will rapidly increase and allow re-training of the models in WP1, which will improve the tracing to a success rate further.

2. Material

Test sites

The data were collected at three test sites across Sweden, one in Norway and one in Finland. The two test sites located in northern Sweden, MDS1 (lat. 64.0° N, long. 20.6° E) and MDS2 (64.3° N, long. 19.8° E), were both covering boreal forest conditions. MDS1 was dominated by Scots pine (*Pinus sylvestris* L.) with a basal-area-weighted mean tree height of 18 m and basal-area-weighted mean diameter of 22.5 cm. MDS2 was dominated by Scots pine with a basal-area-weighted mean tree height of 20.4 m and basal-area-weighted mean tree diameter of 25.8 cm. Data were also collected from two stands at the Living Lab North test site MDS3 in Sweden: MDS-LLN1 (lat. 63.08° N, long. 16.92° E) & MDS-LLN2 (lat. 62.97° N, long. 17.15° E), both covering boreal forest conditions. The Norwegian test site, Oslo, included three stands located in south-eastern Norway (60.79° N 12.09° E) and covered boreal forest conditions. The stand sizes were 4.4, 2.5, and 2.2 ha. They were dominated by Scots pine (*Pinus sylvestris* L.) with basal-area-weighted mean tree heights of 20, 19, and 21 m and volumes of 139, 72, and 147 m³/ha. The Finnish test site Evo consisted of a managed boreal Scots pine-dominated forest stand of ~0.4 ha in size, located in Southern Finland (lat. 61°11'N, long. 25°8'E). The trees were about 50 years old, with a mean density of 430 trees/ha, mean basal area 23.8 m²/ha, and mean basal-area-weighted diameter and height of 28.2 m and 22.8 m, respectively.

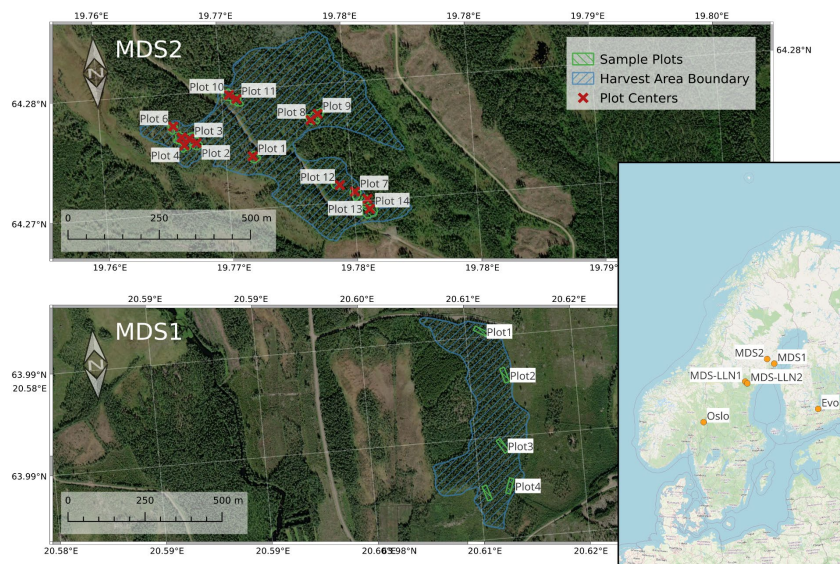


Figure 1 Overview of all the test sites and detailed examples of the two Swedish test sites MDS1 & 2.

Data sets

The data included in the demo are the following:

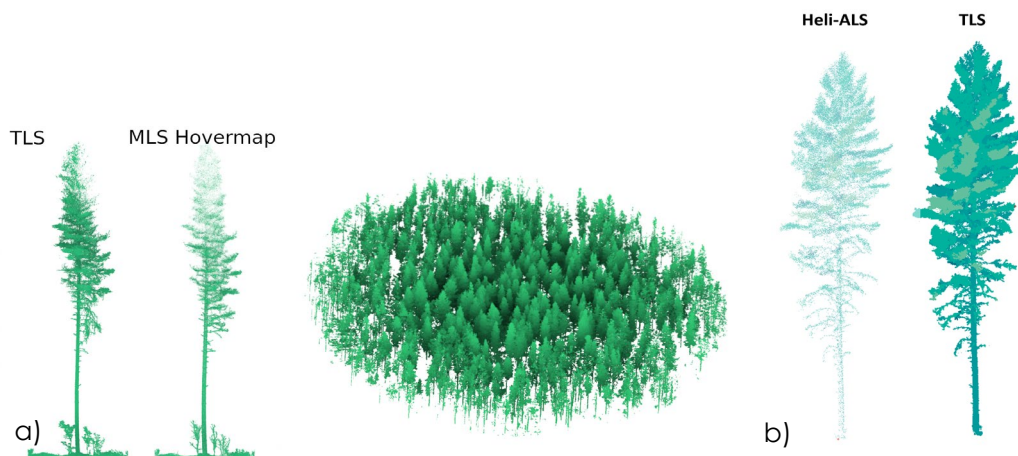
Table 1

Dataset	Description	Sensor	Data Format	Partner
MLS-Sweden	MLS data captured wall-to-wall on a selected stand 2025.	Hovermap	Point clouds *.las/*.laz	SLU
MLS-Norway	MLS data captured wall-to-wall from 3 stands 2024.	GeoSLAM ZEB-Horizon	Point clouds *.las/*.laz	NIBIO
TLS-Sweden	TLS data collected as a sample from the same stands 2025.	Leica RTC360	Point clouds *.las/*.laz	TLS
TLS-Finland	Two-date TLS data collected from a managed Scots pine stand in 09/2021 and 11/2022	Leica RTC360 (2021) Riegl VZ-400i (2022)	Point clouds *.las/*.laz	UEF
HeliALS-Finland	Two-date low-altitude helicopter-borne airborne laser scanning data collected from 28 sample plots and ~2000 Scots pine trees in 06/2021 and 07/2023	Riegl VUX-1HA/ MiniVUX-3UAV/ VQ-840-G (2021) Riegl VUX-1HA/MiniVUX-1DL/ VQ-840-G (2023)	Point clouds *.las/*.laz	UEF, FGI

CT data MDS1,2-Sweden	CT-scanner data from two sites, 23 trees. Collected 2024-2025.	CT	Images *.jpg *.tiff	SLU
CT data MDS3-sawmill-Sweden	CT-scanner data from two stands, ~5800 Scots pine timber logs. RGB-Images and CT-data. Collected 08/2025 ,09/2025.	Mircotec CT Log	Images *.jpg *.tiff	SCA
Log X-ray data, sawmill Norway	X-ray log scanner data from three stands. Collected 09/2024	X-ray		NIBIO

Table 1 Dataset used for the demonstration of tracing methodology.

Examples of the data are shown in Figures 2 a-b.



Figures 2 a-b Examples on the point clouds from the datasets presented in Table 1. a) TLS and MLS from plot 8 at the MDS2 site in Sweden. b) ALS and TLS from Evo, Finland.

Mobile Laser Scanning (MLS)

In the Swedish test sites MDS1 and MDS2, MLS was performed using the Emesent Hovermap ST-X system from (Emesent, Milton, Queensland, Australia). The system has 32 lasers with a 360 degrees horizontal field of view, 40 degrees horizontal field of view. The 360 degrees rotation of the scanner head enables measurements in all directions.

In the Norwegian test site, MLS was conducted using the GeoSLAM ZEB-Horizon system mounted on a backpack-style harness provided by the manufacturer. The ZEB-Horizon uses Simultaneous Localization and Mapping (SLAM) technology to generate 3D point clouds as the operator traverses the terrain. Key performance parameters include a 360° × 270° field of view, a maximum range of 100 m, a scan rate of up to 300,000 points per second, and a system of 16 laser channels/sensors and a relative accuracy is up to 6 mm. The scanner head weighs approximately 1.45 kg, with the datalogger unit around 1.4 kg including battery, making it well-suited for backpack or even hand-held deployment.

Terrestrial Laser Scanning (TLS)

In the Swedish test site MDS1, data collection was carried out in five rectangular plots, each measuring 15 x 50 m². It performed multi-scan TLS data collection by positioning the TLS along the perimeter of the plots every 5 to 10 meters. Each plot required 15 to 20 scans in total. In the Swedish test site MDS2, a variable plot size was used to make the inventory more efficient. The TLS scanning was performed around 14 center locations, with 4-10 TLS scans at each of these locations. Black-and-white reflective targets with positions measured with GNSS were used for references.

In both Swedish sites, the TLS data were collected using a Leica RTC360 system (Hexagon, Heerbrugg, Switzerland), which operates at a wavelength of 1550 nm. The chosen scanning mode provided point spacing of approximately 6 mm at 10 m range. The system captures up to 2 million points per second, with a full 360° horizontal and 300° vertical field of view. The point positioning accuracy was 1.9 mm at 10 m. Post processing of the TLS data was done using the Leica Cyclone software.

The two-date TLS-Finland dataset was collected in September 2021 and November 2022 from a 0.4-ha managed Scots pine stand located in Evo, Finland (Yrttimaa et al. 2025). The 2021 data was collected using a Leica RTC360 scanner, with a scan pattern consisting of 25 individual scanning positions arranged in a regular grid of approximately 16 m spacing across the sample plot. Artificial reference targets were attached to trees to enable co-registration of individual scans as a merged point cloud. The 2021 data was collected using a Riegl VZ-400i scanner, with a scan pattern consisting of 23 individual scanning positions located approximately 11 m apart. The

co-registration of individual scans was conducted automatically on-the-go using the built-in sensor pose estimation capability based on orientation and positioning sensors.

Low-altitude Airborne Laser Scanning (ALS)

The two-date low-altitude HeliALS-Finland data was collected in June 2021 and July 2023 across 28 Scots pine-dominated sample plots located in Evo, Finland. Both datasets were collected using a helicopter-borne three-sensor system consisting of Riegl VUX-1HA (1550 nm), MiniVUX-3UAV/MiniVUX-1DL (905 nm), and VQ-840-G (532 nm). The flight altitude was 80 m and the flight speed was 50 km/h, resulting in a ~3000 pts/m² point density and a 2-cm point spacing on the ground.

Computer Tomography (CT) data

CT images of trees were collected from three Swedish sites, MDS1, MDS2 and MDS3. The first CT dataset is used for the method development and covers the sites MDS1 and MDS2. It was collected in a sister project and was not intended to be used in SingleTree due to copyrights and restrictions. Yet, we experienced limited access (due to copyrights) to the main intended CT-dataset from MDS3 in SingleTree and we succeeded in negotiating a limited access to the dataset from MDS1 and MDS2, that allows us to complete the method development while the negotiations about MDS3 continue.

In the MDS1 & MDS2 sites, a sample of 23 trees were manually felled and bucked into standard lengths. For validation of traceability, the logs were marked with ID numbers that connected them to the location of the standing tree in the forest. The ID number could also be used to connect logs to their original tree stem. The logs were transported to a wood science lab equipped with a high performance computer tomography scanner (CT-scanner). The logs were scanned in the lab with sub-millimeter resolution. These trees were made available to the project in Nov 2025 and are used for method development in SingleTree.

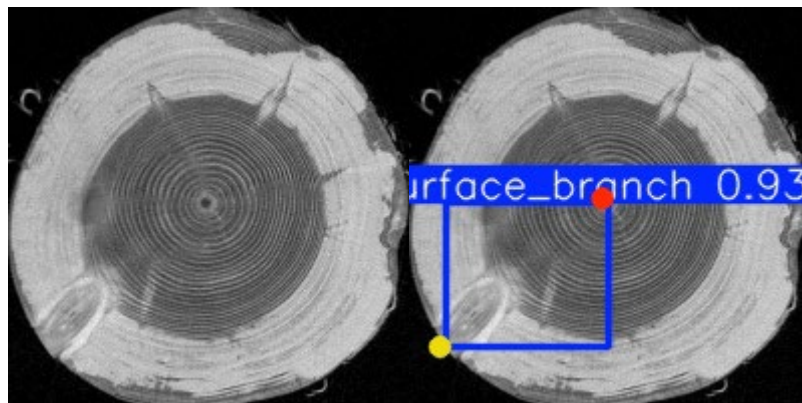


Figure 3 Example on CT scanner images from the Swedish test sites MDS1&2 by the high performance CT-scanner. a) CT-image from a log. b) same CT-image and including the automatically predicted center and branch intersection point.

The two stands MDS3-LLN1 and MDS3-LLN2 comprised 5,800 logs of Scots pine (*Pinus sylvestris*), of which MDS3-LLN1 were harvested between 18 August and 26 August 2025, and CT-scanned between 20 August and 3 September. The trees in MDS3-LLN2 were harvested between 8 September and 12 September 2025, and CT-scanned between 5 September and 23 September. The trees were CT scanned as part of the ordinary operational sawing process at the sawmill, using a Microtec CT LOG scanner, an industrial computed tomography system developed for the sawmilling industry and designed for full-length scanning of roundwood. The system uses a rotating X-ray source and multiple detectors to generate high-resolution three-dimensional images of the internal structure of each log, with a spatial resolution of approximately 1 mm per voxel. The resulting data are stored as encrypted TIFF files, where each centimeter of log length is represented by a separate image slice.

Each log is photographed in connection with the CT-scanning. For each log, three JPG photographs were taken — one side view of the full log and two end-face images where the LogsCom code is visible. The trees were harvested using a harvester equipped with precision GPS in the harvester head, and a LogsCom printer that marked each log end with a unique code. This enables a high degree of traceability and future possibilities to link the CT data with both field and remote sensing data.

At present, the CT-data from MDS3 cannot be accessed or processed in the desired manner due to restrictions imposed by the supplier. An agreement has been reached between the supplier and the user organization that is expected to enable full access to the data in the future, although the timeline for this remains uncertain.

3. Methodology

Concept for fingerprinting using branch patterns

The use of sensors like LiDAR and CT scanners enabled the extraction of parameters that were sufficient to trace the single logs from a standing tree in the forest, to the CT scanner at the sawmill entrance. We limited the search space of trees to the tract level -- typically meaning a population of approximately a few thousand individual trees with a few logs cut from each tree -- which is the level of digital tracing operationally available in 2025 by manual management. This tracing level can also be achieved automatically based on current low-cost GNSS receivers. This enables easy connection of the proposed novel concept with the existing (digital) value chain.

The branch pattern consisted of the identification of branch origins (i.e., the intersections between stem surface and branches) along the stem from detailed point cloud data as presented in (Yrttimaa et al. 2025, Figure 1 A-B). The complex 3D architecture of a tree can thus be condensed into a 2D point pattern depicting branch origins as a function of height above the ground and azimuth angle around the stem (Figure 4F). Similar information of the branching pattern can be obtained when the timber arrives at the factory by automatically identifying knots and their positions in the wood using X-ray CT (Longueaud et al., 2012). By comparing laser scanning-derived and X-ray CT-derived branching patterns, we established a link between harvested trees and their respective timber products. This was tested primarily for pine but 2D X-ray images were considered for spruce as well. As the described approach requires highly accurate point clouds to identify branch origins, we also present an alternative approach more suitable for lower density point cloud data attainable over larger areas. Based on initial experiments, the directional and vertical arrangement of branches along the stem can be derived using low-altitude airborne laser scanning data. Converting individual tree point cloud coordinates from the original 3D Cartesian (X, Y, Z) to 3D Cylinder representation (θ, ρ, h) , where the location of each point is defined as an azimuth angle (θ) and radius (ρ) with respect to a tree orientation axis at a given height (h) (Figure 4 C-D). The data is then rasterized to describe variation in ρ on a plane defined by θ and h (Figure 4 E). Branch segment positions along the stem could then be identified as local raster maxima to indirectly obtain branching arrangement (Figure 4 F). In addition, we tested the feasibility of different point cloud metaproperties to characterize crown structure (Cattaneo et al., 2024) to augment branching arrangement characterization. We tested the robustness of these approaches using point cloud data representing different geometric accuracies and densities: TLS, MLS, and close-range (low-altitude) ALS using a helicopter as a platform.

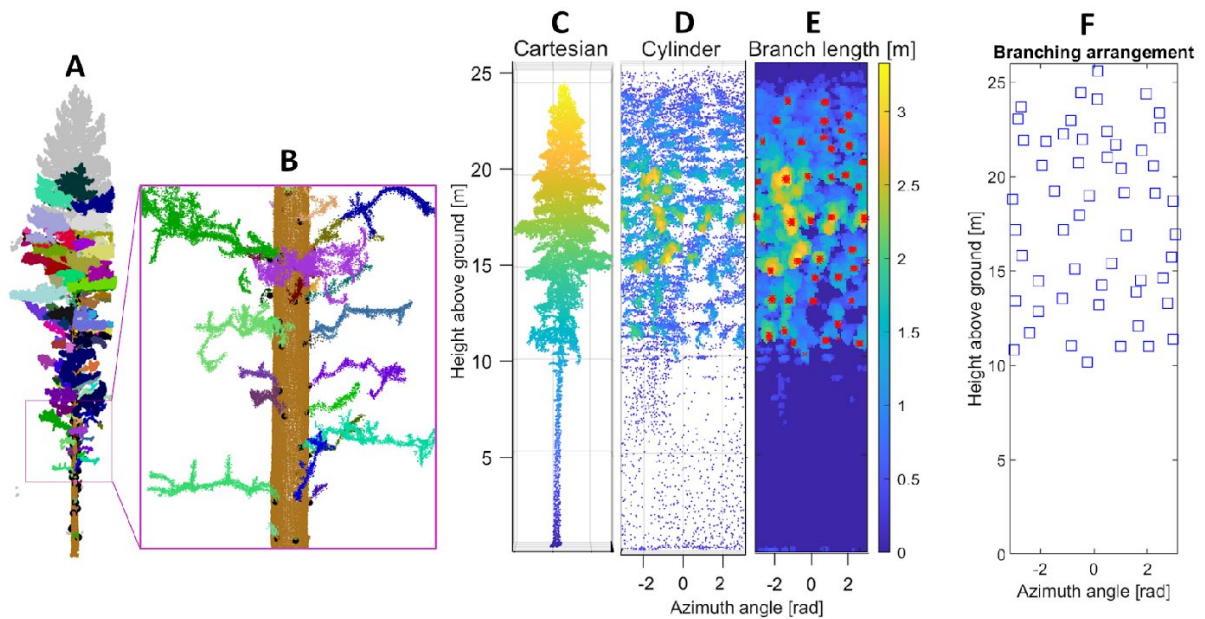


Figure 4 Approaches for deriving branching patterns for trees using different resolution point clouds: 1) Direct identification of branch origins as intersections with the stem surface (A-B) using terrestrial laser scanning data. 2) Indirect assessment of branching arrangement through rasterizing crown directional extent (branch lengths) using close-range airborne or ground-based mobile laser scanning data (C-E). Coordinate conversion from 3D Cartesian to 3D Cylinder representation helps identifying branch locations as local maxima (E). Both approaches result in a 2D pattern of points (F) that can be linked with CT-scanned data at the sawmill.

To investigate whether the proposed approaches would provide the grounds for individual tree fingerprinting and thus for biometric wood traceability, we tested to distinguish individual trees from among a population based on independent point cloud reconstructions A and B (Figure 5). This means that we reconstructed the architecture of trees using two-date or multi-modal point clouds and linked corresponding tree individuals based on the derived tree fingerprints. In case of TLS/MLS data, the fingerprint consisted of a 2D pattern of stem-branch intersections along the stem. For each A-fingerprint, a corresponding B-fingerprinting was searched by analyzing nearest neighbor distances between the stem-branch intersections. For low-altitude ALS data, the derived 2D patterns described branches' lateral distribution along the stem and correspondence between A and B reconstructions was searched by analyzing similarities in the rasterized representations of the cylinder-transformed point clouds using Normalized Cross-Correlation as the measure of similarity.

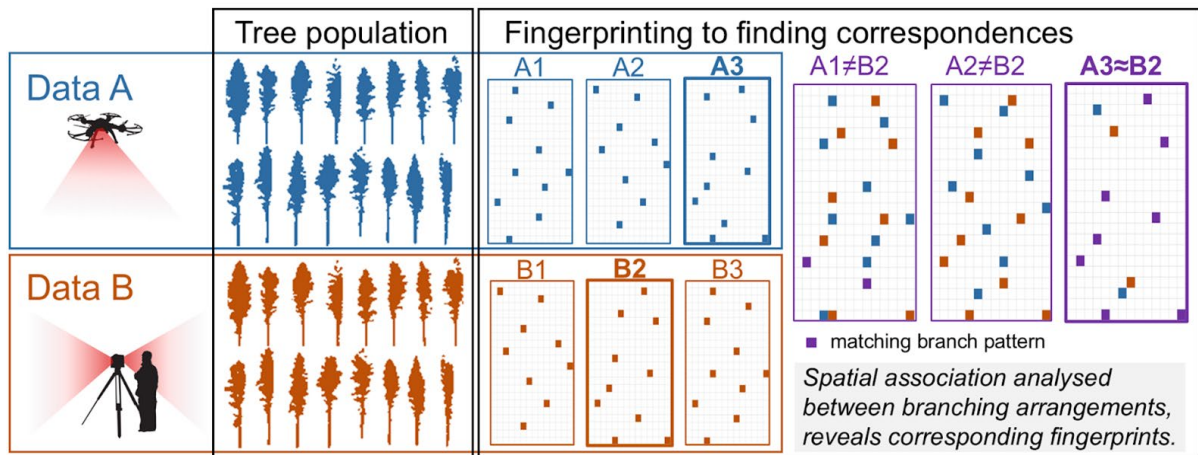


Figure 5. Outline of the methodology used for testing whether trees' unique structural patterns such as the branching architecture as derived from terrestrial or low-altitude airborne laser scanning can be utilized distinguishing individuals within a population, providing the grounds for individual tree fingerprinting.

Refined algorithm for Swedish case study

Based on the methods described in Yrttimaa et al. (2025) we developed a slightly refined algorithm to be tested on the Swedish TLS and MLS datasets. Stem profile estimates were initially extracted for all single trees using the algorithm described in Olofsson et al. (2016). The algorithm resulted in a number of cylinders fitted to the stem of each tree. Based on the cylinder positions, single tree point clouds could be extracted using a circular polygon centered around the base of each tree. Each single tree point cloud was then unwrapped, i.e. a coordinate transform was applied from Cartesian (x,y,z) to cylindrical (θ, h, ρ) coordinates. For each point in the point cloud, ρ is calculated as the horizontal Euclidean distance to the stem orientation axis, θ as the four-quadrant inverse tangent (atan2) based on the x and y components of the point and the stem orientation axis at the same height. h is equal to z . The stem orientation axis was estimated by cubic spline interpolation between the cylinder centers. The tree stems were then represented by a flat surface in (θ, h, ρ) space, See fig 6.

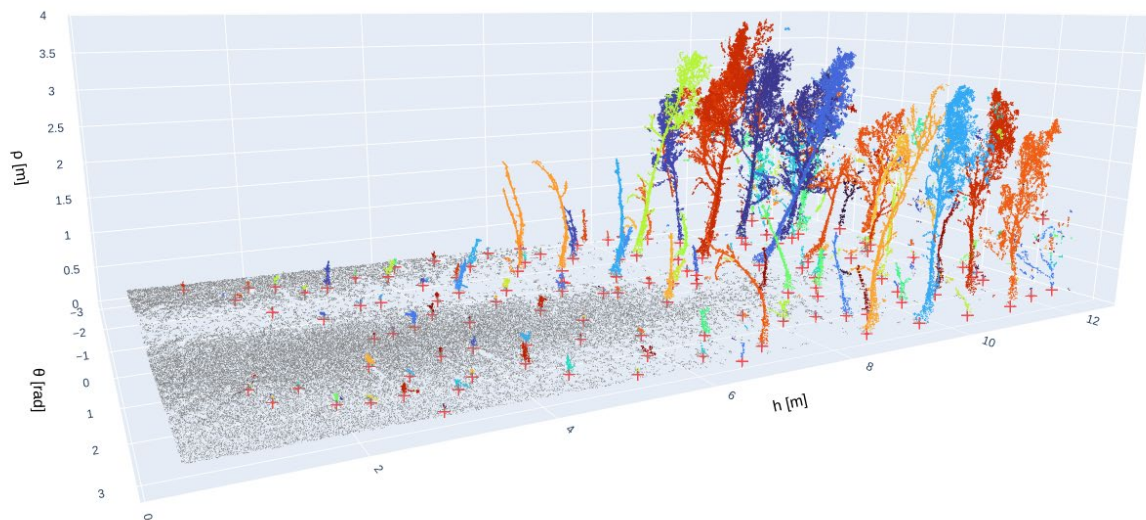


Figure 6. Unwrapped branch surface projected on the θ - h plane.

A “minimum surface grid” was then generated based on the methods described in (Pingel et al, 2013). This grid represented the stem surface, without any branches, analogous to a digital terrain model. We classified points as either “branch” or “stem” based on their radial distance from the minimum surface. To locate the branch intersections, we first identified all points located close to points of the opposite class. This set was then run through a DBSCAN clustering algorithm to differentiate separate branches. The projection of each cluster center onto the minimum surface then defined the branch positions.

We extracted branching patterns for trees within circular areas around each plot center in the MLS and TLS datasets, resulting in 289 MLS/TLS pairs. To determine whether the same individual trees could be identified across both datasets, each MLS tree was compared with every tree in the TLS dataset. During each comparison, the two branching patterns were evaluated by assigning each TLS branch position to its nearest neighbor in the MLS pattern. Branch positions with no neighbor, i.e. those too far from any corresponding point, were excluded from the analysis.

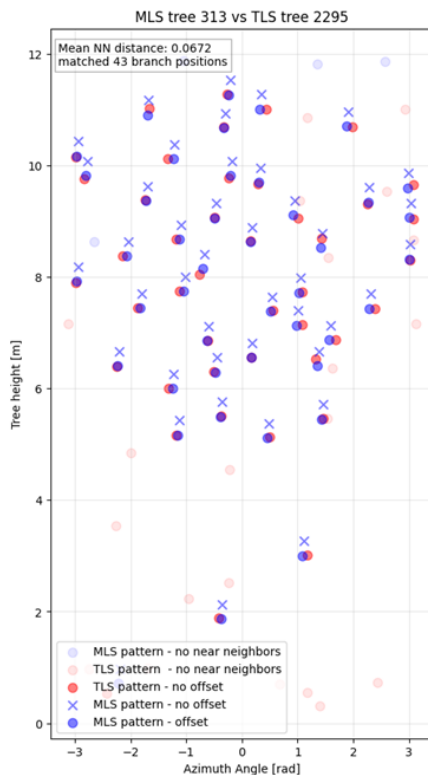


Figure 7. An example of MLS/TLS branch pattern pairs for one tree at the Swedish test site MDS1.

We then computed the mean nearest-neighbor (NN) distance for all matched point pairs. The MLS/TLS pair with the lowest mean NN distance was considered a potential match. To reduce the risk of false matches, we defined an upper limit for acceptable mean NN distances and required a minimum number of matched branch positions, recognizing that in a more operational context, some trees may not have a corresponding match in the other dataset.

In the case study from Sweden, both datasets were georeferenced, which allowed us to use consistent, aligned tree orientations. As a result, branching patterns originating from the same tree should align well. However, in situations where patterns are derived from felled trees, e.g. using CT scanning, this alignment cannot be assumed and the matching process has to be direction- and rotation-invariant. In such cases, before calculating the mean NN distance, we applied offsets to the angular (θ) and vertical (z) coordinates and identified the offsets that minimized the mean NN distances between the two patterns.

4. Results

The methodology was proven successful and depending on the sensors and forest conditions, different results can be presented. As a baseline and overall result, we can report that 52 of 65 trees (80%) were successfully traced in the Finnish test site, using two-date TLS data. More results and details are described below, and divided into different sensor combinations.

Two-date TLS

Experiments using two-date TLS data to investigate whether branching arrangement could serve as a biometric feature for individual trees are presented in Yrttimaa et al. (2025). The findings showed that identifying as few as ten common branches–stem intersections from two independent point cloud reconstructions is sufficient to distinguish individual trees within a population. When comparing the branching arrangements of two randomly selected trees, a few branches may coincide by chance. However, as the number of stem–branch intersections included in the two-dimensional point pattern increases, the likelihood of coincidental similarity rapidly decreases—the minimum requirement appears to be on the order of a dozen intersections, rather than hundreds or thousands.

It should be noted that the population used in the experiment was relatively small, consisting of a single 0.4-ha forest stand with 65 Scots pine trees. Nevertheless, the findings highlight the scale and magnitude of structural information required for biometric recognition of individual trees: it is not necessary to reconstruct the entire tree architecture to differentiate between individuals. A similar level of information content has been demonstrated in linking sawn timber products (boards) to their originating sawlogs, where the distribution of approximately 10-20 knot clusters were sufficient to provide biometric identification (Skog et al. 2017; Zolotarev et al. 2019).

Two-date low-altitude ALS

Using normalized cross-correlation as the similarity measure between raster-based fingerprints, 80% of trees reconstructed in the 2023 HeliALS data could be matched to their corresponding reconstructions in the 2021 dataset. Subtle, natural changes in tree architecture—such as broken branches or branch elongation—did not appear to affect the ability to identify corresponding patterns in the rasterized, cylinder-transformed data. This aligns with the findings from TLS investigations, suggesting that complete reconstruction is not required (i.e., not all branches need to be detected) for biometric recognition of individual trees.

A crucial part of the methodology, however, is the ability to accurately reconstruct stem orientation, which is required for the Cartesian-to-cylindrical coordinate transformation. This imposes certain requirements on both the data and the forest conditions. First, stand density must be sufficiently low—as is typically the case in mature forests where sawlogs are harvested—to ensure adequate visibility of stems from the air. Second, a slightly inclined measurement geometry from the airborne sensor toward the trees enhances stem reconstruction capacity. Nevertheless, it does not appear essential for the stem orientation to be determined exactly, provided that it is captured consistently across both datasets.

We observed that failures in the fingerprinting process were primarily associated with inaccuracies in instance segmentation, leading to anomalies in the rasterized representations of branch lateral distributions and ultimately resulting in unmatchable fingerprints.

MLS data on standing trees accompanied with 2D X-ray data on sawlogs

Some initial results based on data captured along the wood procurement chain suggest that the tree fingerprinting concept is viable for traceability: it was possible to establish links between sawlogs and their originating standing trees by correlating the vertical branching arrangement and stem profile. Since the 3D arrangement of knots could not be reconstructed from 2D X-ray images, we instead analyzed the similarity in the distributions of knot clusters, or whorls, derived either in the forest or at the sawmill. This approach appeared feasible for trees with visible branches in the MLS data; however, sawlogs cut from branchless stems could not be linked based on branching arrangement alone. We found it equally important to detect not only the presence but also the absence of branches in the point cloud data and to link these observations to what is visible in the X-ray images. In particular, regardless of the type of data available from the sawlogs (2D X-ray or CT), we should be able to identify from the X-ray data whether there is wood between the knots and the log surface—a sign of a legacy branch concealed by subsequent wood growth.

Two-date MLS and TLS data

The Swedish case study using two-date MLS and TLS data successfully matched 254 of 275 trees (92%). This contained a mixture of pine and spruce trees, with a dominance of pines. Both the MLS and TLS datasets were dense and lower results can be expected in tough operational conditions with lower visibility or sparser point

clouds. The number of branches needed for finding a successful matching tree in the other dataset varied, from 7 to 97 (Table 2). So for this dataset of 275 trees, 7 uniquely matched branches were sufficient for a successful tracing.

Table 2

Total number of trees	Successful matches	Matched branch pairs
275	254 (92.36%)	28 (mean) 97 (max) 7 (min)

Table 2 Results for tracing of trees using two-date MLS and TLS data. The number of unique branch pairs needed for finding the corresponding tree in the other dataset varied from 7 to 97.

Two-date TLS and CT-scanning data

The matching of TLS and CT-scanning data was not yet successful. Due to the time constraints (we only got access to the spare CT-dataset mid-November 2025), the implementation is not yet completed. We have so far managed to automatically extract branch knot patterns, which seems to work as expected, but the matching procedure is not yet implemented to also handle directional and rotational invariance. Furthermore, the 23 CT-scanned trees were collected in another project with focus on stem defects - hence these trees provide a more challenging test set. We count on having a fully working LiDAR-CT-scanner tracing method implemented in 2026.

5. Conclusions

The methodology of using branch pattern as a unique fingerprint has successfully been implemented and tested on datasets from several sensors of various point densities and properties, in different forests and in 3 different countries. The results are rather robust and solid with successful tracing of approximately 80% - 92%, which is sufficient to use the approach to collect large amounts of additional data automatically. Yet, the pre-processing of datasets is still requiring manual adjustments and the proprietary limitations connected to CT-scanner data are yet to be resolved, before additional steps at larger scales can be completed.

6. Data access

The data is classified as sensitive and will be made available internally to the SingleTree consortium.

References

Cattaneo, N., Puliti, S., Fischer, C. and Astrup, R., 2024. Estimating wood quality attributes from dense airborne LiDAR point clouds. *Forest Ecosystems*, 11, p.100184.

Chiorescu, S., Grönlund, A., 2003. The fingerprint approach: using data generated by a 2-axis log scanner to accomplish traceability in the sawmill's log yard. *For Prod J.* 53, 78–86.

Holmström, E., Raatevaara, A., Pohjankukka, J., Korpunen, H. and Uusitalo, J., 2023. Tree log identification using convolutional neural networks. *Smart Agricultural Technology*, 4, p.100201.

Longuetaud, F., Mothe, F., Kerautret, B., Krähenbühl, A., Hory, L., Leban, J.M. and Debled-Rennesson, I., 2012. Automatic knot detection and measurements from X-ray CT images of wood: a review and validation of an improved algorithm on softwood samples. *Computers and Electronics in Agriculture*, 85, pp.77-89.

Olofsson, K., & Holmgren, J. (2016). Single Tree Stem Profile Detection Using Terrestrial Laser Scanner Data, Flatness Saliency Features and Curvature Properties. *Forests*, 7(9). <https://doi.org/10.3390/f7090207>

Persson, H.J., Puliti, S., Yrttimaa, T., Ghildyal, V., Astrup, R., Holmgren, J., Fischer, C., Cattaneo, N., Vastaranta, M. . Automatic tracing of single trees using close-range laser scanning. *SilviLaser 2025*, Quebec, Canada, 29 Sep-3 Oct, 2025.

Pingel, T. J., Clarke, K. C., & McBride, W. A. (2013). An improved simple morphological filter for the terrain classification of airborne LIDAR data. *ISPRS Journal of Photogrammetry and Remote Sensing*, 77, 21–30. <https://doi.org/10.1016/j.isprsjprs.2012.12.002>

Schraml, R., Hofbauer, H., Petutschnigg, A. and Uhl, A., 2016. On rotational pre-alignment for tree log identification using methods inspired by fingerprint and iris recognition. *Machine Vision and Applications*, 27, pp.1289-1298.

Schraml, R., Charwat-Pessler, J., Petutschnigg, A., & Uhl, A., 2015. Towards the applicability of biometric wood log traceability using digital log end images. *Computers and Electronics in Agriculture*.119, 112-122.

Skog, J., Jacobsson, M., and Lycken, A. (2017). "Traceability and adaptive production in the digital sawmill," *Pro Ligno* 13(4), 162-167

Tzoulis, I., Andreopoulou, Z., 2013. Emerging traceability technologies as a tool for quality wood trade. *Procedia Technol.* 8, 606–611.

Winberg, O., Pyörälä, J., Yu, X., Kaartinen, H., Kukko, A., Holopainen, M., Holmgren, J., Lehtomäki, M., Hyyppä, J., 2023. Branch Information Extraction from Norway Spruce Using Handheld Laser Scanning Point Clouds in Nordic Forests. *ISPRS Open J. Photogramm. Remote Sens.* 9, 100040.

Yrttimaa, T., Junttila, S., Hyyppä, J., Holopainen, M., Wulder, M. A., & Vastaranta, M. (2024). Quantifying architectural uniqueness of Scots pine trees using terrestrial laser scanning: Toward individual tree fingerprinting. *Forestry: An International Journal of Forest Research*. <https://doi.org/10.1093/forestry/cpae058>

Zolotarev, F., Eerola, T., Lensu, L., Kälviäinen, H., Haario, H., Heikkinen, J. and Kauppi, T., 2019, August. Timber tracing with multimodal encoder-decoder networks. In the *International Conference on Computer Analysis of Images and Patterns* (pp. 342-353). Cham: Springer International Publishing.

Glossary

Acronym	Full name
MLS	Mobile laser scanning
TLS	Terrestrial laser scanning
ALS	Airborne laser scanning

CT

Computer tomography
